ACS APPLIED MATERIALS & INTERFACES

Research Article

www.acsami.org

Facile Photochemical Synthesis of Graphene-Pt Nanoparticle Composite for Counter Electrode in Dye Sensitized Solar Cell

Verawati Tjoa,[†,‡,⊥] Julianto Chua,[†,⊥] Stevin S. Pramana,[†] Jun Wei,[‡] Subodh G. Mhaisalkar,[†,§] and Nripan Mathews*[,†,§]

[†]School of Materials Science and Engineering, Nanyang Technological University, Block N4.1, 639798 Singapore

[‡]Singapore Institute of Manufacturing Technology, Tower Block Lv5, 638075 Singapore

[§]Energy Research Institute, Nanyang Technological University, Research Technoplaza, Lv 5, 50 Nanyang Drive,637553 Singapore

Supporting Information

ABSTRACT: A low temperature route to synthesize graphene oxide–Pt nanoparticle hybrid composite by light assisted spontaneous coreduction of graphene oxide and chloroplatinic acid without reducing agent is demonstrated. Analysis indicates the importance of light as energy provider and ethanol as hole scavenger in the formation of small Pt nanoparticles (~3 nm) on graphene oxide as well as graphene oxide reduction. Spray coating was used to deposit the hybrid material as a counter electrode in dye sensitized solar cells (DSCs). An efficiency of 6.77% for the hybrid graphene counter electrode has been obtained, higher than the control device made by low temperature sputtered Pt as counter electrode. Compatibility of the hybrid material with flexible plastic substrates was demonstrated yielding DSCs of an efficiency of 4.05%.

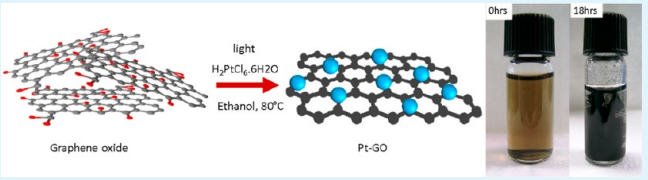

KEYWORDS: *graphene, graphene oxide, metal nanoparticle, platinum, dye sensitized solar cells*

INTRODUCTION

Dye sensitized solar cells (DSCs) are of great interest due to their simple fabrication procedure and high efficiencies.[1] Much of the research in DSCs has focused on synthesis of new dyes, new materials for photoanodes, and new electrolytes.[2−6,43] Alternative materials for counter electrode have received less attention due to the excellent properties of the Pt nanoparticles conventionally deposited through the thermal decomposition of platinum chloride precursor on fluorinated tin oxide (FTO). However, the decomposition requires a high temperature (>400 °C), which is incompatible with plastic substrate. One possible modification that could enable room temperature counter electrode fabrication is the introduction of carbon nanostructures, such as carbon nanotubes, graphene, and other carbon derivatives as a conductive support or catalyst.[5,7−10]

Graphene has attracted much research attention due to its excellent properties such as high charge carrier mobility,[11] high catalytic activity,[12] chemical stability,[8] and high optical transmittance,[13] enabling application in electronics, catalysis, energy storage, and sensing.[14−17] In recent years, graphene based materials have been integrated into DSCs.[18] For example, Nailiang et al. have utilized graphene bridges to enhance charge transport within TiO_2 photoanodes,[19] while Kavan et al. have demonstrated the advantages of employing graphene nanoplatelets in DSC.[12,20] One of the drawbacks in the solution processing of graphene is the final step involving the utilization of high temperature or toxic chemicals (hydrazine) as reducing agents for the conversion of water-soluble graphene oxide (GO) to reduced graphene oxide (rGO).

In this report, we have developed a clean and low temperature method to efficiently reduce insulating GO to conductive rGO while simultaneously decorating Pt nanoparticles on rGO sheet. We have demonstrated its application as a counter electrode in dye sensitized solar cells. The resultant hybrid material has randomly distributed Pt nanoparticles with uniform size of ~3 nm. The reduction process was monitored through optical spectra and XPS characterization. The hybrid material synthesized at different reaction times were extracted and made into counter electrodes by spray coating, which is a scalable process. The DSCs fabricated with hybrid material counter electrodes are shown to possess higher efficiency as compared to "control" DSCs made through other low temperature methods such as spraying Pt nanoparticles (made by heating chloroplatinic acid in ethanol at 80 °C for 3 h, referred as Pt nnp) and sputtered Pt counter electrodes. Finally, incorporation of the hybrid material on plastic substrate has been successfully demonstrated with an efficiency of 4.05%.

EXPERIMENTAL PROCEDURE

Synthesis of Pt–GO. Graphene oxide was produced by modified Hummers' and Offeman method[21] following our previous report.[22] Materials used were graphite powder (SP1, Bay Carbon), sulfuric acid (98%, Sigma Aldrich), sodium nitrate (Sigma Aldrich), potassium permanganate (Sigma Aldrich), and hydrogen peroxide (30%, Sigma Aldrich). Purified and dried GO is then redispersed in a mixture of

Received: March 12, 2012
Accepted: May 30, 2012
Published: May 30, 2012

   dx.doi.org/10.1021/am300437g | ACS Appl. Mater. Interfaces 2012, 4, 3447−3452

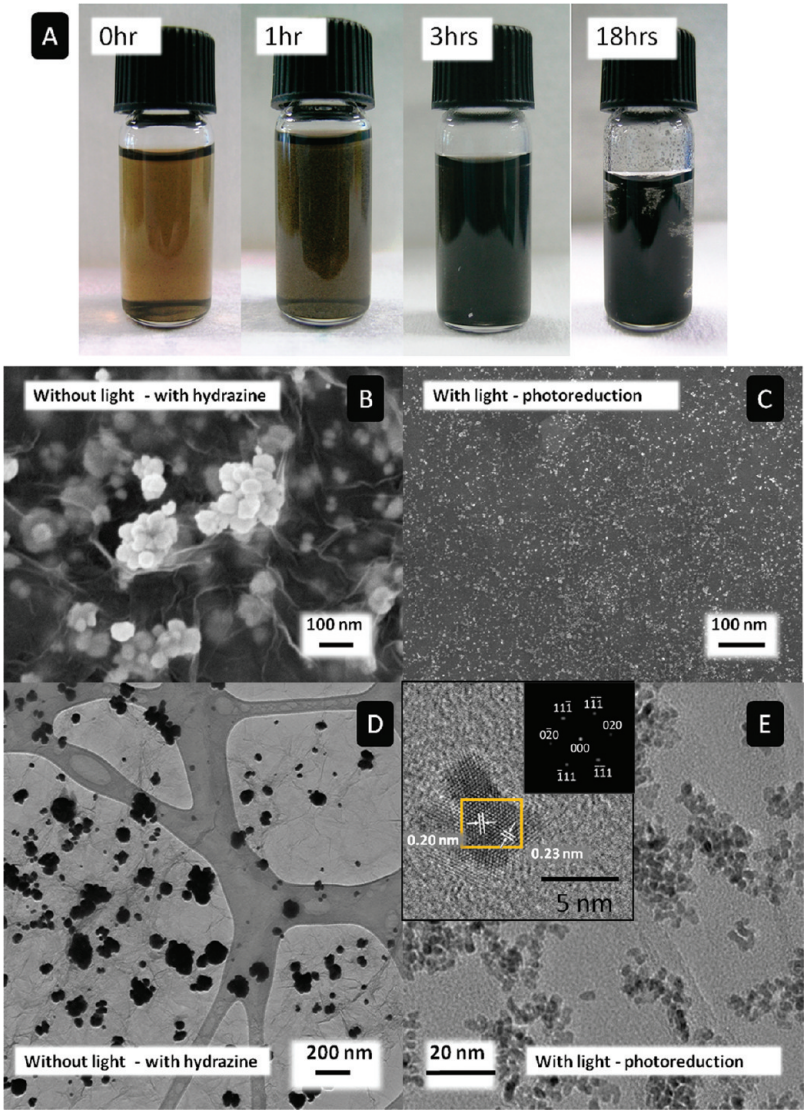

Figure 1. (A) Photograph of PtGO solution at different interval time of 0 h, 1 h, 3 h, and 18 h. (B) SEM image of PtGO made by addition of hydrazine as reduction agent, particle size range is 20−200 nm. (C) PtGO made by light assisted reduction in ethanolic solution; particle size is on average 3 nm. (D) TEM image for PtGO in B. (E) TEM image for PtGO in C, inset showed the HRTEM of the nanoparticle as well as generated FFT image for the particle in the box.

ethanol and DI water (4:1). H_2PtCl_6 solution (Alfa Aesar, 1 mL, 10 mM in ethanol) was then added dropwise to the solution while being vigorously stirred. The solution is then heated to 80 °C, and light from an incandescent bulb (100W, Philips, local intensity 56W/m^2 measured using Daystar PV meter) was used to assist the reaction. The resultant hybrid material was then centrifuged and washed with ethanol several times and redispersed in ethanol. An aliquot of 0.5 mL was sprayed on FTO coated glass substrate to prepare the counter electrode. A similar synthesis method was employed to produce Pt nnp used as counter electrode.

Solar Cell Fabrication. For the preparation of the photoanode, $TiCl_4$ pretreatment is done for 30 min at 70 °C on the FTO glass substrate (TEC15, from NSG). A 10 μm thick mesoporous nanoparticle TiO_2 (Dye-sol 18NRT; particle size, 20 nm) is first screen-printed, followed by a 5 μm thick scattering layer (Solaronix R/SP; particle size, 150 nm). Post $TiCl_4$ treatment is done before dipping in 0.3 mM N719 dye solution for 12 h. The electrolyte used in this experiment is E008 (MPN based, 0.1 M iodine, 1 M PMII, 0.5 M NMB, 0.1 M LiTFSI). For counter electrode, two control samples were made by spraying Pt nanoparticle made by heating chloroplatinic acid in ethanol at 80 °C for 3 h (referred to as Pt nnp in this report) and also by sputtering Pt onto FTO glass. Our study on platinum decorated graphene oxide is done by spraying the solution on FTO coated glass forming a film thickness of around 1μm.

Characterization. A drop of the hybrid suspension was deposited on plasma cleaned silicon and lacey carbon copper grid and left to dry in air before characterization by scanning electron microscopy (FE-SEM, JEOL JSM7600F), X-ray photoelectron spectroscopy (XPS, VG ESCA 220i-XL imaging XPS), and transmission electron microscopy (HR-TEM, JEOL 2100F, Japan). An aliquot of 3 mL was extracted to perform UV−vis optical absorption analysis (Shimadzu 3600, Japan). The film thicknesses of spray coated films were measured using surface profilometer (KLA Tencor alpha stepIQ), and the sheet resistance was measured using a 4-point probe (Advanced Instrument Technology CMT SR 200N, Switzerland). Cyclic voltammogram (CV) was measured using Solartron-analytical, 1470E with Pt foil as counter electrode and SCE as reference electrode in an acetonitrile solution of 1 mM I_2, 10 mM of LiI, and 0.1 M of $LiClO_4$. The cells were illuminated by AAA rated solar simulator (San-Ei Electric, XEC 301S), 1 sun illumination, while I−V characteristics were recorded by Agilent 4155C.

Scheme 1. Schematic of Light Assisted Platinum Salt Reduction on Graphene Oxide Sheet in Ethanolic Solution

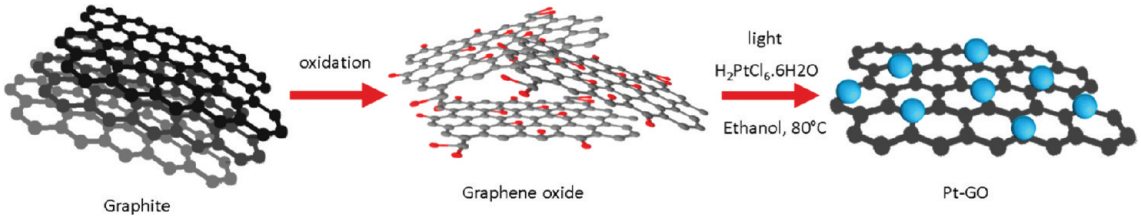

RESULTS AND DISCUSSION

Pt nanoparticles on GO were synthesized by photoreduction of chloroplatinic acid and GO in ethanolic solution and in the presence of light; the resultant hybrid material is referred to as PtGO. The optical image in Figure 1a shows the evolution of color of the same PtGO solution over time (0 to 18 h). The mixture initially appears brownish yellow following the typical color of GO solution. Subsequently, black, web-like sheets started to appear in the solution which increased with time. At the end of 18 h or more, the solution appeared very dark and lost its dispersibility completely. The morphologies and microstructures of the nanocomposites were examined with SEM and TEM. Figure 1b,c compares the PtGO morphology formed by hydrazine reduction and that produced by photoreduction, respectively. Figure 1d,e shows the HRTEM images of PtGO synthesized by hydrazine reduction and by photoreduction for 1 h. Hydrazine was used since it is an effective reducing agent for both GO[16] and chloroplatinic acid.[23] During hydrazine reduction (Figure 1b,d), most of the particles were found to aggregate randomly with irregular shape and size. The size varies from 20 to 200 nm possibly due to the vigorous nature of the reduction. On the other hand, reduction by light produces smaller and uniform particle sizes. As measured through TEM, the average size is 3.2 ± 0.5 nm. The inset of Figure 1e shows an enlarged view of the particle with the selected area electron diffraction (SAED) pattern of the particle highlighted. The Pt nanoparticles were found to crystallize in cubic *Fm*-3*m* (a = 0.392 nm) and were aligned along [101] zone axis. The d-spacing of {111} and {020} were calculated to be 0.23 and 0.20 nm, respectively, from high resolution TEM (HRTEM) and SAED. Elemental analysis by energy dispersive X-ray (EDX) as well as XPS measurements confirms that the particles formed are Pt (Supporting Information, SI 2c,f).

We evaluated the necessity of the various factors involved in the synthesis of the nanocomposite in an attempt to unravel the underlying mechanism. Illumination of graphene oxide and platinum precursor for 18 h in pure DI water resulted in no change in the bright yellow solution (Supporting Information, SI 1), and films cast from the solution remained insulating, indicating the necessity of ethanol.[24,25] It has been reported previously that Pt nanoparticles can be generated from water–alcohol solutions of chloroplatinic acid under illumination.[26−28] The reaction proceeds through the oxidation of alcohols which provides electrons for the reduction process. The chemical functionalities on the surface of graphene oxide have been shown to act as binding sites for metal nanoparticle formation,[22,29] leading to the formation of graphene oxide–Pt hybrid material. Ethanol can also act as a reducing agent in the formation of reduced graphene oxide under these mild conditions.[30,31] Comparison of the TEM images of the nanocomposite (1 h vs 18 h) revealed that the Pt nanoparticles are easily formed and retain their dimensions throughout the illumination period. The Pt nanoparticles in turn catalyze the GO reduction process. Illumination of GO in ethanolic solution without Pt precursor showed no significant change of color after 3 h, indicating a slow reduction process. The role of Pt in accelerating GO reduction processes has been previously observed in ethylene glycol based systems.[32,33] The temperature applied (80 °C) is also critical in accelerating the reduction process. Room temperature syntheses approximately took 5 days to achieve the same level of reduction as 18 h of standard synthesis. As mentioned above, the role of illumination is in the formation of uniform Pt nanoparticles. Conducting the reaction in the darkness resulted in the formation of nonuniform Pt particles and aggregates (>100 nm). The nanoparticle synthesis is shown Scheme 1.

To investigate the gradual transformation of PtGO to form Pt-reduced GO, we performed optical absorption, sheet resistance, and X-ray photoelectron spectroscopy (XPS) spectrum analysis on both solution and thin film samples. Figure 2 shows the absorption spectra taken for H_2PtCl_6–GO solution in ethanol at different time intervals. The solution prior to photoreduction has two absorption peaks at 228 nm (corresponding to $\pi \rightarrow \pi^*$ transition of C=C bond) and a shoulder peak at around 300 nm (corresponding to $n \rightarrow \pi^*$ transition in carbonyl conjugation). The peak at 228 nm gradually shifts to 247 nm after 1 h of illumination, 255 nm after 3 h, and finally to 269 nm after 18 h of illumination. From previous reports, reduced graphene oxide has been reported to have an absorbance at around 270 nm.[34] Similarly, the shoulder peak also gradually shifts from 300 to 350 nm as the reaction time increases. The gradual shift of the curve is due to increasing conjugative interaction and signifies the restoration

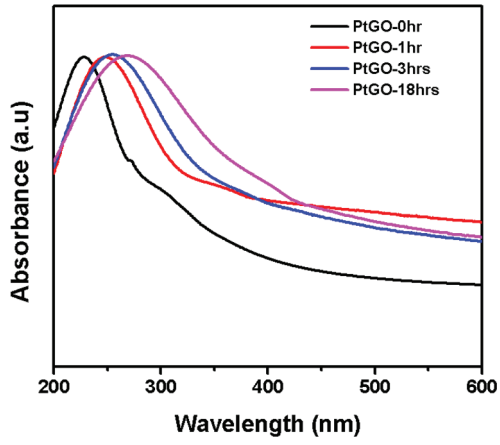

Figure 2. UV–vis absorbance for graphene oxide and chloroplatinic acid in ethanolic solution at different time intervals ranging from 0 to 18 h.

dx.doi.org/10.1021/am300437g | ACS Appl. Mater. Interfaces 2012, 4, 3447−3452

of the graphene sp^2 structure, which also suggests removal of oxygen functionality.[35]

Sheet resistance measurements were made on spray coated thin film samples (thickness is around 0.8−1.0 μm) on glass substrate. The value gradually decreases from >300 MΩ/sq to 3.21 kΩ/sq. This value is comparable to a hydrazine reduced PtGO sheet resistance value of 11.39 kΩ/sq (Supporting Information, SI 3). Meanwhile, hydrazine reduced GO has a sheet resistance value of 15.52 kΩ/sq, indirectly indicating that the Pt nanoparticles may improve conductivity in the composite material. Another way to characterize the reduction degree of GO is by analyzing the oxygen and carbon peaks in XPS. Figure 3 showed a survey and high resolution scan for

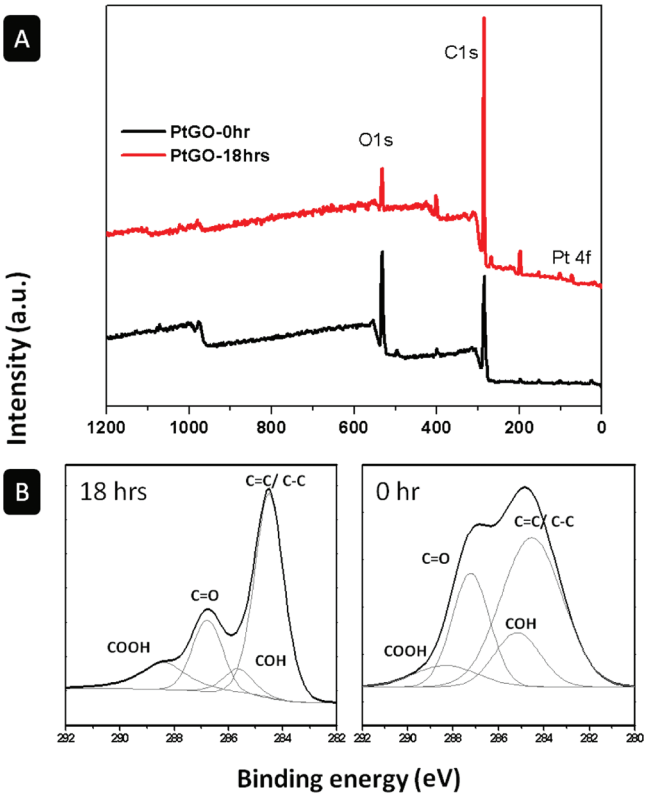

Figure 3. X-ray photoelectron spectroscopy for PtGO at 0 and 18 h: (A) survey scan and (B) high resolution scan for PtGO and GO.

PtGO at 0 and 18 h of illumination. Oxygen functionalities that could be detected in graphene oxide include hydroxyl (286.6 eV), carbonyl (287.9 eV), and carboxylate (289.1 eV).[36,37] The intensity of these peaks decrease with illumination time, while the intensity of the peak associated with conjugated carbon at 284.5 eV increases. Further analysis shows a carbon to oxygen ratio of 2.6 and 12.8 for PtGO-0 h and PtGO-18hrs, respectively, confirming the removal of oxygen group in GO.[38,39] The XPS results also confirm the presence of Pt nanoparticles. A high resolution Pt4f XPS scan of PtGO-18hrs showed a small peak at around 75 eV which may suggest the presence of intermediate products Pt (+2) (Supporting Information, SI 2f) or possible interaction between graphene sheet and the Pt nanoparticle.[40]

In order to demonstrate practical applications utilizing this composite, a series of dye sensitized solar cells were fabricated with PtGO as counter electrode. Each of the solutions was spray coated on FTO glass to a thickness of 1 μm as measured by surface profilometer. A 1 μm thickness of the films was used because it was the lowest thickness where consistent results could be produced. At this thickness, there is sufficient coverage and continuity of the film on the substrate, providing consistency. Figure 4 shows the $J-V$ characteristic of

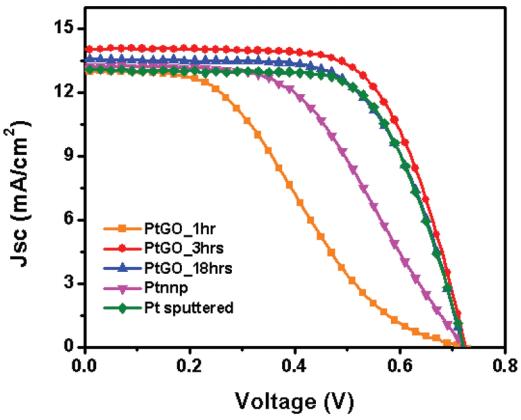

Figure 4. $J-V$ characteristic of DSC made of PtGO counter electrode at different reaction time and reference cell of Pt nanoparticle, Pt sputtered on FTO as comparison.

representative DSCs prepared under various synthesis conditions. The results are tabulated in Table 1 for easy reference.

Table 1. Photovoltaic Characteristic of DSC with PtGO Counter Electrode on FTO

	V_{oc} (V)	J_{sc} (mAcm^{-2})	FF (%)	η (%)
Pt−GO-1h	0.71	13.0	35.8	3.31
Pt−GO-3hrs	0.72	14.1	66.9	6.77
Pt−GO-18hrs	0.71	13.5	65.1	6.26
Pt nnp	0.72	13.2	50.9	4.85
Pt sputtered	0.72	13.1	67.2	6.29

An open circuit voltage (V_{oc}) of 0.71 V, a short-circuit current density (J_{sc}) of 13.0 mA cm^{-2}, a fill factor (FF) of 35.85, and conversion efficiency (η) of 3.31% were obtained for PtGO-1hr. On the other hand, the V_{oc}, J_{sc}, FF, and η for PtGO-3hrs were 0.72 V, 14.1 mA cm^{-2}, 66.9, and 6.77% and for PtGO-18hrs were 0.71 V, 13.5 mA cm^{-2}, 65.1, and 6.26%, respectively. From the result, we can observe an increasing trend of the efficiency along with the reaction time. There is also a significant difference in FF of PtGO-1hr compared to the PtGO-3hrs and PtGO-18hrs. Interestingly, J_{sc} and FF of the PtGO-3hrs cell are found out to be slightly higher than the PtGO-18hrs cell.

In general, the counter electrode of the DSC should possess both good conductivity and high catalytic activity. Both of these factors vary during the reduction of PtGO. The poor performance exhibited by PtGO-1hr may be attributed to the inadequate restoration of the sp^2 network which leads to inefficient charge transport and high sheet resistance. For longer reduction times (3 and 18 h), the poor conductivity is no longer a hindrance as demonstrated by the high photocurrent densities and fill factors in the devices. Previous studies have pointed out that the oxygen functional group in carbonaceous material may play a strong catalytic role.[9,41] With increasing reaction time, more functional groups are removed from the graphene, possibly leading to lower catalytic activity for PtGO-18hrs as compared to PtGO-3hrs. This could

dx.doi.org/10.1021/am300437g | ACS Appl. Mater. Interfaces 2012, 4, 3447−3452

be the possible reason behind the slight dip in the DSC efficiencies when photoreduction times are increased from 3 to 18 h. To investigate the catalytic performance of the counter electrodes, cyclic voltammetry was conducted in a three electrode system with Pt foil as counter electrode and SCE as reference electrode. The result is presented in Figure 5. Two

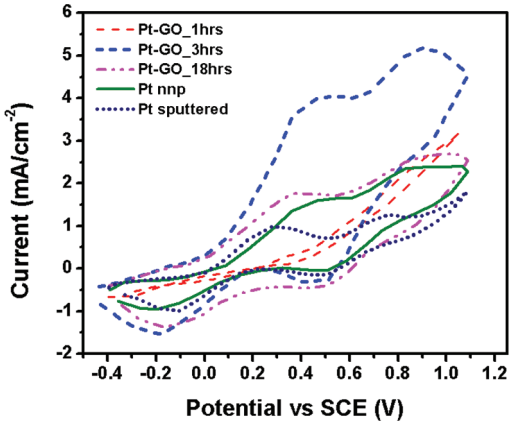

Figure 5. Cyclic voltammetry of PtGO-1hrs, PtGO-3hrs, PtGO-18hrs, Pt nanoparticle sprayed on FTO, and Pt sputtered on FTO. The scan rate is 50 mV/s.

pairs of peaks are observed corresponding to oxidation (positive peaks) and reduction (negative peaks) of the iodide/triiodide species. The reduction processes occurring are ($I_3^- + 2e^- \rightarrow 3I^-$) and ($3I_2 + 2e^- \rightarrow 2I_3^-$).[42] In general, PtGO-3hrs and PtGO-18hrs were found to exhibit large redox current density as compared to PtGO-1hr and the sputtered Pt counter electrode with PtGO-3hrs showing the best catalytic activity. The results imply that, at short reduction times (1 h), low conductivity creates a bottleneck in the performance of the PtGO; while in the case of longer time periods (18 h), the improvement in conductivity could not sufficiently compensate for the decrease in catalytic activity. Optimization of conductivity and catalytic properties gives better efficiency for PtGO-3hrs as compared to the sputtered Pt cells. The good FF observed for the PtGO electrodes also suggest that this approach has potential for counter electrode application in DSC. The ambient nature of the fabrication process as well as the scalable nature of the spray deposition shows that this new material is compatible with high throughput production on flexible substrates.

We have also demonstrated the ability of the Pt−GO material to be incorporated onto flexible substrate (ITO/PET, sheet resistance of 200Ω/sq) as shown in Supporting Information, SI 4. The device showed good performance reaching an efficiency of 4.05%. Generally, the efficiency of cells made using flexible substrate were lower than that fabricated on rigid FTO, attributable in part to the higher sheet resistance of the flexible substrate. The cell performance is plotted in Figure 6, with the inset showing the tabulated result of the cells. The V_{oc}, J_{sc}, FF, and η for PtGO on ITO/PET substrate were 0.71 V, 10.62 mA cm^{-2}, 53.37, and 4.05%, respectively. The stability of the Pt−GO electrode formed on plastic substrate was tested continuously for 100 electrochemical cycles and displayed no significant change in the catalytic activity, indicating good adhesion of the composite material (Supporting Information, SI 5).

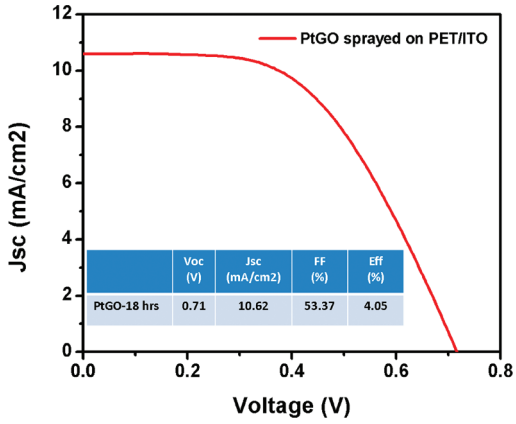

Figure 6. *J*−*V* characteristic of DSC made of flexible PtGO counter electrode. Inset showed the tabulated cell performance.

CONCLUSION

We have presented low temperature light assisted coreduction of both graphene oxide and Pt nanoparticles in ethanol−water mixtures. The reduction was found to effectively remove the oxygen functionalities and recover the conductivity of graphene sheet. The advantages of our method are (1) clean synthesis and spontaneous coreduction of PtGO hybrid material involving no toxic chemical and (2) a low temperature solution processable method compatible with flexible plastic substrate. The applicability of the hybrid material to perform as DSC counter electrode has also been demonstrated. An efficiency of 6.77% is achieved for PtGO hybrid counter electrode, higher than 6.29% obtained through sputtering of platinum. In addition, the hybrid material has also been integrated on flexible substrate as counter electrode, and an efficiency of 4.05% was obtained. This promising performance suggests that PtGO hybrid synthesized by photoreduction may be an excellent alternative for low temperature based counter electrode in DSC.

ASSOCIATED CONTENT

Supporting Information

Additional optical figure, TEM images, tabulated sheet resistance results, XPS results, optical image of flexible counter electrode made by PtGO, and cyclic voltammetry stability measurement for flexible counter electrode. This information is available free of charge via the Internet at http://pubs.acs.org/.

AUTHOR INFORMATION

Corresponding Author

*E-mail: Nripan@ntu.edu.sg.

Author Contributions

⊥These authors contributed equally to this work.

Notes

The authors declare no competing financial interest.

ACKNOWLEDGMENTS

The authors would like to express gratitude to Dr. Zhang Zheng and Mr. Daniel Li Teng Hui for the help in XPS measurement

REFERENCES

(1) O'Regan, B.; Gratzel, M. *Nature* **1991**, *353*, 737.

(2) Wang, M.; Chamberland, N.; Breau, L.; Moser, J.-E.; Humphry-Baker, R.; Marsan, B. t.; Zakeeruddin, S. M.; Grätzel, M. *Nat. Chem.* **2010**, *2*, 385.
(3) Mathews, N.; Varghese, B.; Sun, C.; Thavasi, V.; Andreasson, B. P.; Sow, C. H.; Ramakrishna, S.; Mhaisalkar, S. G. *Nanoscale* **2010**, *2*, 1984.
(4) Dou, X.; Sabba, D.; Mathews, N.; Wong, L. H.; Lam, Y. M.; Mhaisalkar, S. *Chem. Mater.* **2011**, *23*, 3938.
(5) Wu, M.; Lin, X.; Wang, T.; Qiu, J.; Ma, T. *Energy Environ. Sci.* **2011**, *4*, 2038.
(6) Hagfeldt, A.; Boschloo, G.; Sun, L.; Kloo, L.; Pettersson, H. *Chem. Rev.* **2010**, *110*, 6595.
(7) Lee, W. J.; Ramasamy, E.; Lee, D. Y.; Song, J. S. *ACS Appl. Mater. Interfaces* **2009**, *1*, 1145.
(8) Wang, X.; Zhi, L.; Mullen, K. *Nano Lett.* **2007**, *8*, 323.
(9) Roy-Mayhew, J. D.; Bozym, D. J.; Punckt, C.; Aksay, I. A. *ACS Nano* **2010**, *4*, 6203.
(10) Murakami, T. N.; Grätzel, M. *Inorg. Chim. Acta* **2008**, *361*, 572.
(11) Novoselov, K. S.; Geim, A. K.; Morozov, S. V.; Jiang, D.; Zhang, Y.; Dubonos, S. V.; Grigorieva, I. V.; Firsov, A. A. *Science* **2004**, *306*, 666.
(12) Kavan, L.; Yum, J. H.; Grätzel, M. *ACS Nano* **2011**, *5*, 165.
(13) Nair, R. R.; Blake, P.; Grigorenko, A. N.; Novoselov, K. S.; Booth, T. J.; Stauber, T.; Peres, N. M. R.; Geim, A. K. *Science* **2008**, *320*, 1308.
(14) Fowler, J. D.; Allen, M. J.; Tung, V. C.; Yang, Y.; Kaner, R. B.; Weiller, B. H. *ACS Nano* **2009**, *3*, 301.
(15) Gómez-Navarro, C.; Weitz, R. T.; Bittner, A. M.; Scolari, M.; Mews, A.; Burghard, M.; Kern, K. *Nano Lett.* **2009**, *9*, 2206.
(16) Goki, E.; Manish, C. *Adv. Mater.* **2010**, *22*, 2392.
(17) Lu, G.; Ocola, L. E.; Chen, J. *Appl. Phys. Lett.* **2009**, *94*, 083111.
(18) Guo, C. X.; Guai, G. H.; Li, C. M. *Adv. Energy Mater.* **2011**, *1*, 448.
(19) Yang, N.; Zhai, J.; Wang, D.; Chen, Y.; Jiang, L. *ACS Nano* **2010**, *4*, 887.
(20) Kavan, L.; Yum, J.-H.; Nazeeruddin, M. K.; Grätzel, M. *ACS Nano* **2011**, *5*, 9171.
(21) Hummers, W. S.; Offeman, R. E. *J. Am. Chem. Soc.* **1958**, *80*, 1339.
(22) Tjoa, V.; Jun, W.; Dravid, V.; Mhaisalkar, S.; Mathews, N. *J. Mater. Chem.* **2011**, *21*, 15593.
(23) Vidal-Iglesias, F. J.; Solla-Gullón, J.; Rodriguez, P.; Herrero, E.; Montiel, V.; Feliu, J. M.; Aldaz, A. *Electrochem. Commun.* **2004**, *6*, 1080.
(24) Lightcap, I. V.; Kosel, T. H.; Kamat, P. V. *Nano Lett.* **2010**, *10*, 577.
(25) Huang, X.; Zhou, X.; Wu, S.; Wei, Y.; Qi, X.; Zhang, J.; Boey, F.; Zhang, H. *Small* **2010**, *6*, 513.
(26) Sakamoto, M.; Fujistuka, M.; Majima, T. *J. Photochem. Photobiol., C: Photochem. Rev.* **2009**, *10*, 33.
(27) Cameron, R. E.; Bocarsly, A. B. *Inorg. Chem.* **1986**, *25*, 2910.
(28) Einaga, H.; Harada, M. *Langmuir* **2005**, *21*, 2578.
(29) Goncalves, G.; Marques, P. A. A. P.; Granadeiro, C. M.; Nogueira, H. I. S.; Singh, M. K.; Grácio, J. *Chem. Mater.* **2009**, *21*, 4796.
(30) Dreyer, D. R.; Jia, H.-P.; Bielawski, C. W. *Angew. Chem., Int. Ed.* **2010**, *49*, 6813.
(31) Dreyer, D. R.; Murali, S.; Zhu, Y.; Ruoff, R. S.; Bielawski, C. W. *J. Mater. Chem.* **2011**, *21*, 3443.
(32) Xu, C.; Wang, X.; Zhu, J. *J. Phys. Chem. C* **2008**, *112*, 19841.
(33) Li, Y.; Gao, W.; Ci, L.; Wang, C.; Ajayan, P. M. *Carbon* **2010**, *48*, 1124.
(34) Li, D.; Muller, M. B.; Gilje, S.; Kaner, R. B.; Wallace, G. G. *Nat. Nanotechnol.* **2008**, *3*, 101.
(35) Huang, L.; Liu, Y.; Ji, L.-C.; Xie, Y.-Q.; Wang, T.; Shi, W.-Z. *Carbon* **2011**, *49*, 2431.
(36) Compton, O. C.; Jain, B.; Dikin, D. A.; Abouimrane, A.; Amine, K.; Nguyen, S. T. *ACS Nano* **2011**, *5*, 4380.
(37) Pham, V. H.; Cuong, T. V.; Hur, S. H.; Oh, E.; Kim, E. J.; Shin, E. W.; Chung, J. S. *J. Mater. Chem.* **2011**, *21*, 3371.
(38) Schniepp, H. C.; Li, J.-L.; McAllister, M. J.; Sai, H.; Herrera-Alonso, M.; Adamson, D. H.; Prud'homme, R. K.; Car, R.; Saville, D. A.; Aksay, I. A. *J. Phys. Chem. B* **2006**, *110*, 8535.
(39) Yang, D.; Velamakanni, A.; Bozoklu, G.; Park, S.; Stoller, M.; Piner, R. D.; Stankovich, S.; Jung, I.; Field, D. A.; Ventrice, C. A., Jr.; Ruoff, R. S. *Carbon* **2009**, *47*, 145.
(40) Wang, Y.; Liu, J.; Liu, L.; Sun, D. *Nanoscale Res. Lett.* **2011**, *6*, 241.
(41) Trancik, J. E.; Barton, S. C.; Hone, J. *Nano Lett.* **2008**, *8*, 982.
(42) Huang, Z.; Liu, X.; Li, K.; Li, D.; Luo, Y.; Li, H.; Song, W.; Chen, L.; Meng, Q. *Electrochem. Commun.* **2007**, *9*, 596.
(43) Chua, J.; Mathews, N.; Jennings, J. R.; Yang, G.; Wang, Q.; Mhaisalkar, S. G. *Phys. Chem. Chem. Phys.* **2011**, *13*, 19314−19317.